

Shape transition of strain-induced InAsSbP islands at liquid-phase epitaxy on InAs (100) substrate: from pyramid to semiglobe

K. M. Gambaryan^{1,*}, V. M. Aroutiounian¹, A. K. Simonyan¹, and T. Boeck²

¹ *Department of Physics of Semiconductors and Microelectronics, Yerevan State University,
A. Manoukian Str. 1, Yerevan, 0025, Armenia*

² *Leibniz Institute for Crystal Growth (IKZ), Max Born-Str. 2, Berlin, 12489, Germany*

Received 10 October, 2008

* E-mail: kgambaryan@ysu.am

Abstract

The Liquid Phase Epitaxy (LPE) technique is used for self-assembled InAsSbP-based strain-induced islands formation on InAs(100) substrates. Here we show that such islands, as they decrease in size, are undergoing a shape transition. As the islands volume decrease, the following succession of shape transitions has been detected: truncated pyramid, {111} faceted pyramid, {111} and partially {105} faceted pyramid, completely unfaceted “pre-pyramid”, which gradually evolve to semiglob. The morphology, size, shape and composition of these objects are investigated by scanning electron microscope (SEM) and Energy Dispersive X-Ray Analysis (EDXA) technique. A critical size (~550 nm) of the InAsSbP-based strain-induced islands shape transformation from “pre-pyramid” to semiglobe is experimentally detected and, in addition, theoretically explained and calculated. Proposed theoretical approach has been also employed and tested for Si_{1-x}Ge_x model system islands grown on a Si(001) substrate. It is shown that for both materials the theoretically calculated values of the critical size coincide with the experimentally obtained data.

PACS: 61.46.-w; 62.23.-c; 64.70.Nd; 81.05.Ea; 81.15.Lm

Key Words: Liquid Phase Epitaxy, Self-Assembled, Strain-Induced, III–V Compounds
Semiconductors, Pyramids, Quantum Dots

1. Introduction

In the last years self-organizing epitaxial growth mechanisms have been utilized for the fabrication of strongly strained coherent islands and quantum dots for their future application in modern semiconductor micro- and nanostructures and devices. Among quantum dots, wires and islands fabrication techniques, the self-organized Stranski–Krastanov method [1] is an important one by which dislocation-free dots, elongated islands, and wires can be produced. By this method, when the islands are in minimum size, quantum dots are circular. Indeed, above a certain critical thickness, the growth mode switches from the conventional layer-by-layer (i.e., two-dimensional, 2D) to a 3D growth mode due to the accumulation of elastic energy in the strained layer that, first, partially relaxes by spontaneously nucleating small islands of the strained material and, later, by creating misfit dislocations. The key parameters of islands are the shape, size distribution, strain and composition which can modify the electronic and optical properties of the final product using in a semiconductor device. Precise control of the growth process is required in order to produce highly regular mono-disperse island arrays. However, many aspects of especially III–V ternary and quaternary compound islands (and then quantum dots) formation and evaluation and other scientific and technological problems are still poorly understood. There is a well-developed understanding of island nucleation [2,3] and subsequent coarsening [4] for the simple case where islands grow with a fixed shape. But in several cases, bimodal island size distributions have been observed, inconsistent with classic coarsening [5–8]. Recently it has been shown that the bimodal size distribution is directly related to a change in shape of the growing islands [7]. The precise nature of this shape transition has been the subject of some discussion [7,8]. But it is clear that the shape change is closely related to the problem of obtaining the uniform island size distribution [8], a key issue for potential applications of these islands in nanoscale devices. Ge and Si–Ge on Si(001) have been widely used as model systems for understanding the islands formation and heteroepitaxy [9–11]. In particular, a misfit strain drives the formation of epitaxial islands, and there is a great interest in exploiting such “self-assembled quantum dots” in nanoscale technology. This system exhibits many remarkable features. As a model system, it suggests that heteroepitaxy is surprisingly complex. Ge islands were first observed by Mo et al. [9] as {105}-faceted rectangular pyramids. A rich body of subsequent work showed that, in equilibrium, small islands are square pyramids, while larger islands develop a more complex multifaceted shape [7] after passing through a first-order shape transition [2,8,10]. The similar shape transition for InGaAs alloy quantum dots grown on a GaAs substrate has been also detected [12]. Several technological growth methods have been applied for the fabrication of such type of islands, in particular, molecular beam epitaxy (MBE) [12], chemical vapor deposition [13], migration enhanced epitaxy (MEE) [12], ultrahigh vacuum magnetron sputtering epitaxy (UHV–MSE) [14], and liquid-phase epitaxy [11,15].

Narrow band-gap III–V semiconductor materials such as InAs, GaSb, InSb, and their alloys are particularly interesting and useful since they are potentially promising to access mid- and far-infrared wavelength regions. They should provide the next generation of LEDs, lasers, and photodetectors for applications such as infrared gas sensors, in molecular spectroscopy, thermal imaging, and thermophotovoltaic cells (TPV) [16].

In this paper we present the experimental and theoretical studies of InAsSbP-based strain-induced islands shape transition at LPE on InAs(100) substrates.

2. Results and Discussion

It is generally accepted that, in contrast to MBE, CVD and MOCVD techniques, LPE is an equilibrium growth technique and produces epitaxial materials of the highest crystalline perfection containing a few point defects and impurities and is therefore well-suited for optoelectronic devices fabrication. However, it is generally thought to be unsuitable for the growth of quantum wells, strain-induced islands, and quantum dots. The main arguments against conventional LPE relate to the high initial growth rate which results in poor thickness control and reproducibility for thin layer epitaxy. However, at appropriate crucible modifications the LPE technique has been successfully employed to grow quantum-well heterostructure lasers [17], multilayer III–V structures with quantum size effects [18], and quantum dots [15, 19–23].

2.1. Experimental Procedures

The samples were grown by LPE using a slide-boat crucible. Consequently, LPE grown islands on (100) or (001) oriented surfaces exhibit a similar shape for an extended concentration range mainly consisting of truncated pyramids with a nearly constant aspect ratio of the island base to the island height of two. To ensure a high purity of the epitaxial layers, the entire growth process is performed under pure hydrogen atmosphere. The InAs(100) substrates have a 11 mm diameter, are undoped, with a background electron concentration of $n=2\times10^{16}$ cm⁻³. The quaternary alloy InAs_{0.742}Sb_{0.08}P_{0.178} used here is conveniently lattice-matched to InAs. We have previously used this alloy for the fabrication of quantum dots [14], thermophotovoltaic (TPV) cells, and mid-infrared diode heterostructures [16].

To expect quaternary strain-induced islands formation, we used arsenic undersaturated and antimony supersaturated liquid phase. To provide a lattice mismatch up to 2% between the InAs substrate and InAsSbP epilayer, we used mole fractions of $X_{\text{InAs}} = 0.0195$, $X_{\text{Sb}} = 0.1228$, and $X_{\text{InP}} = 1.7\times10^{-4}$ in the growth melt. The LPE growth solution components – undoped InAs, undoped InP, and Sb (6N) were solved in a In (7N)-solution which has been first homogenized for one hour at $T=580^\circ\text{C}$ and then for two hours at LPE initial growth temperature of $T=550^\circ\text{C}$. Then the quaternary

liquid phase was brought in contact with the InAs substrate. To initiate the growth of islands, we used an over-saturation by decreasing the initial growth temperature up to 2°C using the slower ramp rate.

We have performed the Scanning Electron Microscopy and Energy Dispersive X-Ray Analysis (SEM-EDXA-FEI Nova 600-Dual Beam) technique to study the strain-induced InAsSbP-based islands, in particular, their composition, elastic strength (lattice mismatch ratio), and shape transformation. The quaternary InAs_{1-x-y}Sb_xP_y pyramids compositions were found at values of x < 4 at % and y < 2 at %. Our investigations show that InAsSbP strain-induced islands, as they decrease in size, are undergoing a shape transition. As the islands volume decreased, the following succession of shape transitions has been detected (Fig. 1a–f): truncated pyramid, {111} faceted pyramid, {111} and partially {105} faceted pyramid, completely unfaceted “pre-pyramid”, which gradually evolved to semiglob.

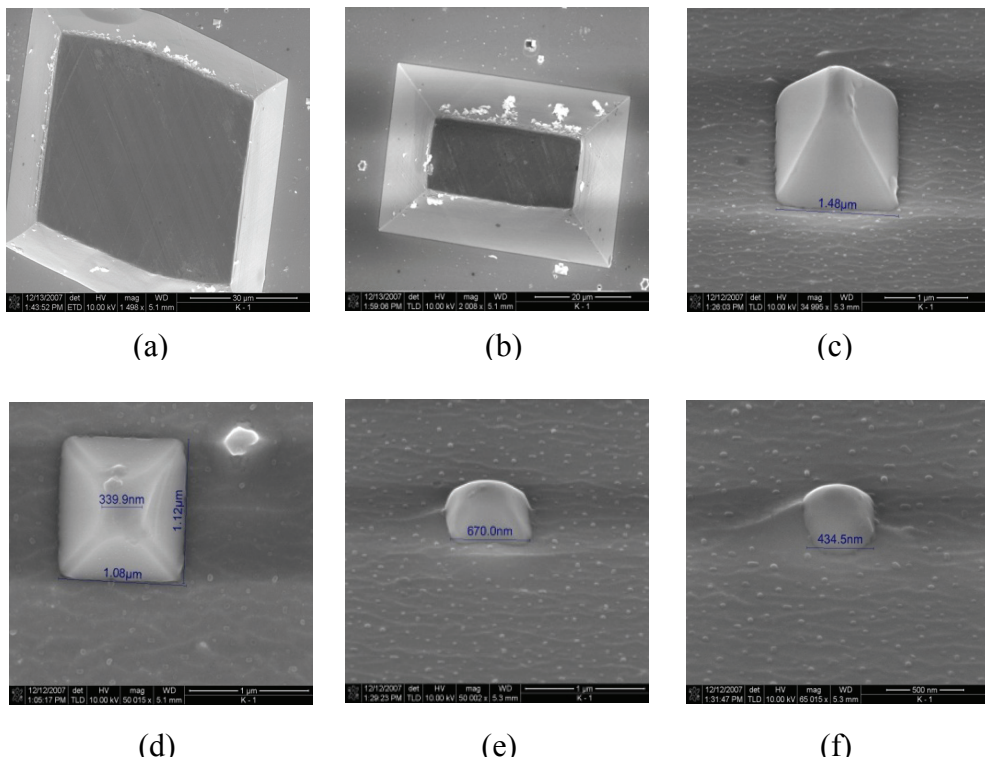


Figure 1. The self-assembled InAsSbP-based strain-induced islands grown by LPE on the InAs (100) substrate and their evolution from a truncated pyramid to a semiglobe.

On the base of EDXA measurements data the strength (lattice-mismatch ratio) of up to 1% is calculated and also shown that the islands size becomes smaller when the lattice mismatch decreases. Because the difference in lattice parameter of the substrate and islands is large enough, we assume that the growth process is consistent with the Stranski-Krastanov mechanism. However,

we are unable to confirm the presence of a wetting layer without a transmission electron microscopy (TEM) study. From the SEM measured values of the “smallest” pyramid base length (670 nm – Fig. 1e) and of the globe-shape island diameter (435 nm – Fig. 3f) we can conclude that the critical size of shape transformation from “pre-pyramid” to semiglobe is within 450 – 650 nm. More detailed experimental determination of this critical size is described in [15]. Indeed, when checking the whole substrate surface, we did not find any pyramid having a size smaller than ~550 nm.

2.2. Theory

In order to theoretically explain and quantitatively calculate the critical size of the island shape transformation from pyramid to semiglobe, the following theoretical approach is performed. Here we derive an explicit approximation for the energy, which provides good explanation of island shape transition. Generally, the smallest “pre-pyramid” shape consists of four {111} and eight {105} facets at (100) or (001) directed substrate. According to the SEM measurements, for our system the total value of {105} facets surface is negligibly small in comparison with the {111} facets surface. That is why we assume that our island is a truncated pyramid with the width s , length t and height h , in the x -, y - and z -directions, respectively. We assume also that the pyramid is symmetric and the edge is at an angle θ to the substrate. We take as our energy reference the InAs(100) substrate plus InAsSbP quaternary island strained to match with the substrate in the x - and y -directions, and free to relax in the z -direction.

The island total energy can be written as

$$E = E_S + E_R + E_V, \quad (1)$$

where E_S is the extra surface and interface energy, E_R is the energy change due to the elastic relaxation, and E_V is the volume energy. In particular,

$$E_S = st(\gamma_i + \gamma_t - \gamma_s) + 2(s+t) [h\gamma_e \csc \theta - h \cot \theta (\gamma_t + \gamma_s - \gamma_i)/2], \quad (2)$$

where γ_s , γ_t , and γ_e are the surface energy (per unit area) of the substrate and of the island top and edge facets, respectively, and γ_i is the island–substrate interface energy [22].

For the case of coherent Stranski–Krastanow growth, where the strained material wets the surface before forming islands, $\gamma_t = \gamma_s$ and $\gamma_i = 0$, so the surface energy term becomes

$$E_s = 2(s+t) h \Gamma, \quad (3)$$

where $\Gamma = \gamma_e \csc \theta - \gamma_s \cot \theta$.

Generally,

$$\gamma_s = \frac{1}{2} C_{ij} \varepsilon_i \varepsilon_j, \quad (4)$$

where C_{ij} ($i, j = 1, \dots, 6$) are the elastic modulus and $\varepsilon = \Delta a/a$ is the relative strain. In order to calculate the energy of elastic relaxation, we assume that the composition of multicomponent island does not change in the z -direction and that the strain ε is constant, i.e., $\varepsilon_{xz} = \varepsilon_{yz} = 0$. For the crystals with a cubic symmetry

$$\gamma_s = \left(\frac{1}{2} C_{11} \frac{\Delta a^2}{a^2} + \frac{1}{2} C_{44} \frac{\Delta a^2}{a^2} \right) d_{\text{wet}}, \quad (5)$$

where d_{wet} is the wetting layer thickness.

Thus, the energy of elastic relaxation is determined by [2]

$$E_R = -\frac{1}{2} \int dx dx' \chi_{ij}(x-x') f_i(x) f_j(x'), \quad (6)$$

where x and x' are two-dimensional (2D) vectors, $f_i = \partial_j \sigma_{ij}$ is the force density at the surface, and χ is the elastic Green's function of the surface, which describes the linear response to an applied force. Here $\sigma_{ij} = \sigma_b h(x) \delta_{ij}$ is the 2D islands stress tensor, $\sigma_b = C_{ij} \frac{\Delta a}{a}$ is the xx - or yy -component of the bulk stress of islands uniformly strained to the substrate x and y lattice constants, and allowed to relax in z , and $h(x)$ is the height (thickness) of the island at the position x .

The analytically evaluated result of integral (6) at the surface Green's function of an isotropic solid [22] can be written as

$$E_R^{\text{pyramid}} = -2ch^2 \left[s \ln\left(\frac{t}{\phi h}\right) + t \ln\left(\frac{s}{\phi h}\right) \right], \quad (7)$$

where $c = \sigma_b^2 (1-\nu)/2\pi\mu$ and $\phi = e^{-3/2} \cot \theta$. Here $\nu = \lambda / (2(\lambda + \mu))$ is the Poisson ratio, μ and λ are the Lame coefficients, and $h = \frac{b_1 - b_2}{2} \tan \theta$, $t = s = \frac{b_1 + b_2}{2}$, where b_1 and b_2 are the lengths of truncated pyramid base and top, correspondingly.

Thus, the pyramid total energy can be written as

$$E^{\text{pyramid}} = E_S + E_R = -\frac{c}{2}(b_1 - b_2)^2(b_1 + b_2) \tan^2 \theta_p \left(\ln \frac{b_1 + b_2}{b_1 - b_2} + \frac{3}{2} \right) + (b_1^2 - b_2^2) \left(\frac{1}{\cos \theta_p} \gamma_e - \gamma_s \right), \quad (8)$$

where θ_p is the angle between the pyramid edge and the substrate surface.

For calculation of the glob-shape island total energy we perform the following approach. Using expression (7) at $b_2 = 0$, $b_1 = s = t = D$ and $h = D/2$, where D is the diameter of semiglobe, the elastic relaxation and surface energy of the glob-shape island can be written as

$$E_R^{\text{globe}} = -cD^3 \left(\frac{3}{2} - \ln \frac{\cot \theta_G}{2} \right) \quad (9)$$

$$E_S^{\text{globe}} = \frac{\sigma S_{\text{globe}}}{2} = \frac{\sigma \pi D^2}{2}, \quad (10)$$

where σ is the density of the globe surface energy and θ_G is the angle between the tangent to the semiglobe and the substrate surface.

The island's volume energy is determined as a sum of the chemical potentials of each component, and since at the critical volume, when the island changes the shape from pyramid to semiglobe, the number and type of components are the same, then we have

$$E_V^{\text{pyramid}} = E_V^{\text{globe}}. \quad (11)$$

Finally, the energy equilibrium condition can be written as

$$E_S^{\text{pyramid}} + E_R^{\text{pyramid}} = E_S^{\text{globe}} + E_R^{\text{globe}}, \quad (12)$$

or in bare view

$$\begin{aligned} & -\frac{c}{2}(b_1 - b_2)^2(b_1 + b_2) \tan^2 \theta_p \left(\ln \frac{b_1 + b_2}{b_1 - b_2} + \frac{3}{2} \right) + (b_1^2 - b_2^2) \left(\frac{1}{\cos \theta_p} \gamma_e - \gamma_s \right) = \\ & = -cD_{\text{cr}}^3 \left(\frac{3}{2} - \ln \frac{\cot \theta_G}{2} \right) + \frac{\sigma \pi D_{\text{cr}}^2}{2}, \end{aligned} \quad (13)$$

where D_{cr} is the critical size (diameter) when the island shape is changed from truncated “pre-pyramid” to semiglobe.

For the calculation of numerical values of some parameters, in particular, the elastic modulus and the density of surface energy and other parameters for the InAsSbP quaternary alloys, we employed the following linear approximation:

$$P(\text{InAs}_{1-X-Y}\text{Sb}_X\text{P}_Y) = P^{\text{InAs}}(1 - X - Y) + X P^{\text{InSb}} + Y P^{\text{InP}}. \quad (14)$$

The appropriate calculated values for $\text{InAs}_{1-x-y}\text{Sb}_x\text{P}_y$ islands grown on InAs(100) substrate and $\text{Si}_{1-x}\text{Ge}_x$ islands grown on Si(001) substrates, as well as known from the literature data for InAs, InSb, InP, Si and Ge are presented in Table 1.

Table 1.

	InAs	InSb	InP	$\text{InAs}_{1-x-y}\text{Sb}_x\text{P}_y$ $x=0.04; y=0.02$	Si	Ge	$\text{Si}_{1-x}\text{Ge}_x$ $x=0.3$	$\text{Si}_{1-x}\text{Ge}_x$ $x=0.5$
$C_{11} \times 10^{-12}$, dyn/cm ²	8.329	6.669	10.11	8.267	1.657	1.26	1.538	1.458
$C_{12} \times 10^{-12}$, dyn/cm ²	4.526	3.645	6.61	4.538	0.639	0.44	0.5793	0.5395
$C_{44} \times 10^{-12}$, dyn/cm ²	3.959	3.626	4.56	3.9564	0.796	0.677	0.7603	0.7365
d_{wet} , nm	- - -	1.266	4.866	14.29	- - -	3.234	8.581	6.767
$\sigma \times 10^7$, J/cm ²	752	- - -	- - -	~ 752	310	181	219	245

It is well known that the transmission electron microscopy (TEM) is the most useful technique for determination of the wetting layer thickness. The measured values for some III–V compound semiconductors are presented in Fig. 2. In order to determine the wetting layer thickness (d_{wet}) for quaternary InAsSbP used in this work, as well as for SiGe-based islands, the following approach has been performed. At first, using the exponential function, we perform the mathematical approximation of experimental data and create the analytic expression (15), which describes the dependence of wetting layer thickness (in monolayers) versus the relative lattice mismatch ratio (in percent):

$$d_{\text{wet}} = 25.232 e^{-0.3584 \frac{\Delta a}{a}}, \quad (15)$$

The approximation accuracy is equal to $R^2 = 0.9988$. The corresponding calculated values for d_{wet} are also presented in Table 1.

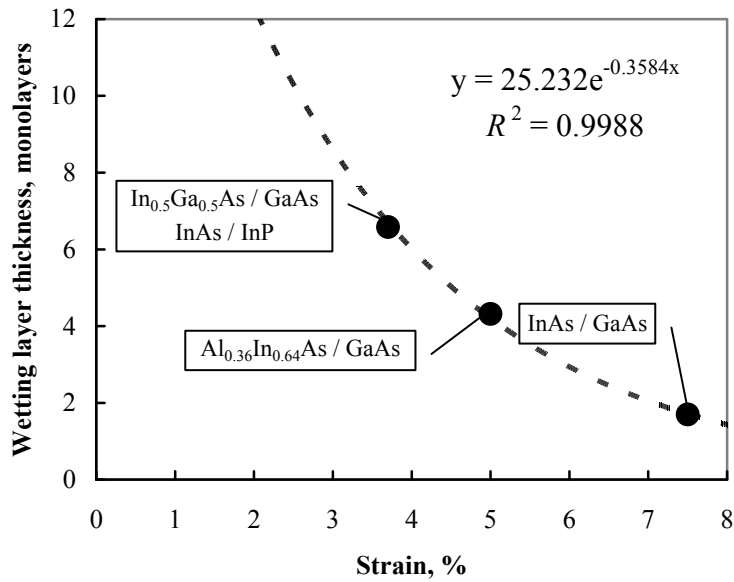


Figure 2. Dependence of the wetting layer thickness on strain; circles – experimental data, dashed line – mathematical approximation.

Thus, solving the equation (13) at $b_1=670 \text{ nm}$, $b_2=150 \text{ nm}$, $\gamma_e=5 \times 10^{-5} \text{ J/cm}^2$ [23],

$$\lambda = \frac{1}{5}(2C_{11} + 3C_{12} + 4C_{44}) = 9.195 \times 10^{12} \text{ dyn/cm}^2, \quad \mu = \frac{1}{10}(8C_{44} + C_{11} - C_{12}) = 3.537 \times 10^{12} \text{ dyn/cm}^2,$$

$$\gamma_s = \left(\frac{1}{2}C_{11} \frac{\Delta a^2}{a^2} + \frac{1}{2}C_{44} \frac{\Delta a^2}{a^2} \right) d_{\text{wet}} = 3.42 \times 10^{-6} \text{ J/cm}^2, \quad v = 0.361, \quad \sigma_b = 1.65 \times 10^{10} \text{ dyn/cm}^2, \quad c = 0.784 \text{ J/cm}^3,$$

$\theta_G = 25^\circ$, $\theta_P = 40^\circ$, $\frac{\Delta a}{a} = 2 \times 10^{-3}$, the critical size (diameter) of $d_{\text{cr}} \approx 550 \text{ nm}$ for InAsSbP islands

shape transformation from truncated “pre-pyramid” to semiglobe is determined. This value exactly coincides with the experimental result (Fig. 1e–f).

We have performed the same calculations also for Si_{1-x}Ge_x model system islands grown on the Si(001) substrate at $x = 0.3$ and $x = 0.5$.

$$\text{At } x=0.3, \quad b_1=95 \text{ nm}, \quad b_2=5 \text{ nm}, \quad \gamma_e=8 \times 10^{-5} \text{ J/cm}^2 [23], \quad \lambda=1.57 \times 10^{12} \text{ dyn/cm}^2,$$

$$\mu=7.046 \times 10^{11} \text{ dyn/cm}^2, \quad \gamma_s=14.4 \times 10^{-6} \text{ J/cm}^2, \quad v=0.345, \quad \sigma_b=1.92 \times 10^{10} \text{ dyn/cm}^2, \quad c=5.495 \text{ J/cm}^3,$$

$$\theta_G=4^\circ, \quad \theta_P=70^\circ, \quad \frac{\Delta a}{a}=1.25 \times 10^{-2}, \text{ coupled with the parameters presented in Table 1, the critical}$$

diameter is equal to $d_{\text{cr}} \approx 70 \text{ nm}$. And for $x=0.5$, $b_1=45 \text{ nm}$, $b_2=15 \text{ nm}$, $\gamma_e=8 \times 10^{-5} \text{ J/cm}^2$ [23],

$$\lambda=1.49 \times 10^{12} \text{ dyn/cm}^2, \quad \mu=6.8 \times 10^{11} \text{ dyn/cm}^2, \quad \gamma_s=2.96 \times 10^{-6} \text{ J/cm}^2, \quad v=0.343,$$

$\sigma_b = 3.04 \times 10^{10}$ dyn/cm², $c = 14.22$ J/cm³, $\theta_G = 9^\circ$, $\theta_P = 65^\circ$, $\frac{\Delta a}{a} = 2 \times 10^{-2}$, $d_{cr} \approx 40$ nm. These both calculated values also coincide with experimentally obtained results [14].

3. Summary

Thus, the Liquid Phase Epitaxy (LPE) technique was used for self-assembled InAsSbP-based strain-induced islands formation on InAs(100) substrates. A shape transition was detected with decreasing island volume. A critical size of quaternary islands shape transformation from “pre-pyramid” to semiglobe is experimentally detected and, in addition, theoretically explained and calculated. Proposed theoretical approach has been also employed and tested for Si_{1-x}Ge_x model system islands grown on the Si(001) substrate. It is shown that for both materials the theoretically calculated values for the critical size coincide with the experimentally obtained data.

Acknowledgments

The authors wish to thank Prof. R. Fornari for fruitful discussions and M. Schulze for SEM-EDXA measurements. This work was carried out in the framework of Armenian National Governmental Program for Nano-Electronics and Nano-Technology and ISTC Grant A-1232.

References

1. I. Stranski and L. Krastanow, *Math.-Naturwiss.* **146**, 797 (1938).
2. I. Daruka, J. Tersoff, and A.-L. Barabasi, *Phys. Rev. Lett.* **82**, 2753 (1999).
3. J. Tersoff and F. K. LeGoues, *Phys. Rev. Lett.* **72**, 3570 (1994).
4. M. Zinke-Allmang, L. C. Feldman, and M. H. Grabow, *Surf. Sci. Rep.* **16**, 377 (1992).
5. C. M. Reaves et al., *Appl. Phys. Lett.* **69**, 3878 (1996).
6. A. Ponchet et al., *Appl. Phys. Lett.* **67**, 1850 (1995).
7. G. Medeiros-Ribeiro et al., *Science* **279**, 353 (1998).
8. F. M. Ross, J. Tersoff, and R. M. Tromp, *Phys. Rev. Lett.* **80**, 984 (1998).
9. Y.-W. Mo, D. E. Savage, B. S. Swartzentruber, and M. G. Lagally, *Phys. Rev. Lett.* **65**, 1020 (1990).
10. J. Tersoff, B. J. Spencer, A. Rastelli, and H. von Kanel, *Phys. Rev. Lett.* **89**, 196104 (2002).
11. M. Hanke, M. Schmidbauer, D. Grigoriev, H. Raidt, P. Schafer, R. Kohler, A.-K. Gerlitzke, and H. Wawra, *Phys. Rev. B* **69**, 075317 (2004).
12. N. Liu, J. Tersoff, O. Baklenov, A. L. Holmes, Jr., and C. K. Shih, *Phys. Rev. Lett.* **84**, 334 (2000).
13. F. M. Ross, J. Tersoff, and R. M. Tromp, *Phys. Rev. Lett.* **80**, 984 (1998).

14. A. Rastelli, H. Von Kanel, B. J. Spencer, and J. Tersoff, *Phys. Rev. B* **68**, 115301 (2003).
15. K. M. Gambaryan, V. M. Aroutiounian, T. Boeck, M. Schulze, and P. G. Soukiassian, *J. Phys. D: Appl. Phys.* **41**, 162004 (2008); K. M. Gambaryan, V. M. Aroutiounian, T. Boeck, M. Schulze, and P. G. Soukiassian, *Armenian Journal of Physics* **1**, 28 (2008).
16. V. A. Gevorkyan, V. M. Aroutiounian, K. M. Gambaryan, A. H. Arakelyan, I. A. Andreev, L. V. Golubev, and Yu. P. Yakovlev, *Solid State Electronics* **52**, 339 (2007).
17. E. A. Rezek, N. Holonyak Jr., and B. K. Fuller, *J. Appl. Phys.* **51**, 2402 (1980).
18. D. Z. Garbuzov, E. V. Zhuravkevich, A. I. Zhmakin, Yu. N. Makarov, and A. V. Ovchinnikov, *J. Crystal Growth* **110**, 955 (1991).
19. A. Krier, Z. Labadi, and A. Hammiche, *J. Phys. D: Appl. Phys.* **32**, 2587(1999).
20. A. Krier, X. L. Huang, and A. Hammiche, *Appl. Phys. Lett.* **77**, 3791 (2000).
21. A. Krier and X. L. Huang, *Physica E* **15**, 159 (2002).
22. J. Tersoff and R. M. Tromp, *Phys. Rev. Lett.* **70**, 2782 (1993).
23. K. L. Safonov, V. G. Dubrovskii, N. V. Sibirev, and Yu. V. Trushin, *Technical Physics Letters* **33**, 490 (2007).